Available online at www.sciencedirect.com
ScienceDirect
Journal of the European Ceramic Society 26 (2006) 3407–3413
www.elsevier.com/locate/jeurceramsoc

Long term oxidation behaviour of liquid phase pressureless sintered SiC–AlN ceramics obtained without powder bed

Giuseppe Magnani [a,*], Leandro Beaulardi [b]

[a] *ENEA, Technical and Scientific Division for Advanced Physics Technologies, Via dei Colli 16, 40136 Bologna, Italy*
[b] *ENEA, Technical and Scientific Division for Materials and New Technologies, Via Ravegnana 186, 48018 Faenza, Italy*

Received 29 June 2005; received in revised form 26 October 2005; accepted 30 October 2005
Available online 6 January 2006

Abstract

This paper describes the results of the investigation of the oxidation behaviour of 50 wt.% SiC–50 wt.%AlN composites obtained by means of pressureless sintering with Y_2O_3 as sintering-aid and without using a powder bed to limit the weight loss. Sintered bodies show high density (>98%T.D.) and the microstructure reveals a matrix composed by SiC–AlN solid solution with $Y_{10}Al_2Si_3O_{18}N_4$ as grain boundary phase. This material exhibits a parabolic oxidation kinetic in the temperature range 1200–1500 °C. Long term oxidation (200 h) induces the formation of a protective oxide scale, composed by mullite, cristobalite and yttrium disilicide, up to 1400 °C. At higher temperature (1500 °C), SiC oxidation behaviour changes from "passive" to "active" and the oxide layer consequently shows porosity due to the formation of gaseous species like SiO and CO.

Keywords: Sintering; Oxidation resistance; SiC; AlN

1. Introduction

Silicon carbide (SiC) and aluminium nitride (AlN) form a 2H solid solution which has received considerable attention owing to its high potential for application in chemically aggressive environments.[1,2] The SiC–AlN composites were preferably sintered by hot pressing in inert[3] or nitrogen atmosphere[4] or in vacuum.[5] Gas pressure sintering (GPS) was also developed,[6] while pressureless sintering with liquid phase forming additives (LPS) was partially inhibited due to the large amount of evaporation loss associated with various chemical reactions.[7] In this case a powder bed was normally used to limit the effects of the decomposition of species like yttria, added as sintering aids to the SiC–AlN mixture, and alumina.[8,9] In a previous paper, we have already demonstrated that high density SiC–AlN ceramics can successfully be obtained by liquid phase pressureless sintering without using a powder bed.[10]

In addition, many studies reported in literature were aimed to the investigation of the correlation between mechanical properties (toughness, flexural strength) and microstructural features of hot pressed SiC–AlN ceramics in order to understand the role of 2H solid solution and βSiC-αSiC transformation from the toughening point of view.[11–14] In contrast, only few studies can be found on the oxidation behaviour of this material.[15–17] Main experimental results in this field put in evidence that oxidation resistance depends on factors like SiC/AlN ratio, sintering procedure, sintering-aids. In particular, Lavrenko et al.[15] demonstrated that hot pressed 50 wt.% SiC–50%AlN ceramics were more oxidation resistant than 20 wt.% SiC–80 wt.% AlN due to the formation of an outer layer of mullite that ensured high protection against oxidant environments. These authors performed oxidation tests only for 6 h, while long term oxidation tests were conducted by Sciti et al.[16] on pressureless sintered AlN-rich materials (78 wt.%) for 100 h and by Pan et al.[17] on hipped SiC-rich materials (85 wt.%) for 30 h. AlN-rich materials showed a low oxidation resistance at 1400 °C due to the porosity and defects located in the brittle surface scale containing free alumina, while SiC-rich materials exhibited a better oxidation resistance.

To our knowledge, there are not studies applied to the investigation of the oxidation behaviour of 50 wt.%SiC–50 wt.%AlN composites obtained by liquid phase pressureless sintering. In

* Corresponding author. Fax: +39 051 6098187.
E-mail address: giuseppe.magnani@bologna.enea.it (G. Magnani).

0955-2219/$ – see front matter © 2005 Elsevier Ltd. All rights reserved.
doi:10.1016/j.jeurceramsoc.2005.10.005

Table 1
Characteristics of the starting powders

Powder	Purity (wt.%)	Specific surface area (m^2/g)	Particle size (μm)
α-SiC	>97.0	15.6	0.48
AlN	>97.0	3.6	0.1–0.5
Y_2O_3	99.9		

this study, we characterized the long term (200 h) oxidation behaviour of SiC–AlN ceramics manufactured by liquid phase pressureless sintering without using a powder bed and we compared our material with analogous materials obtained with other sintering routes from the high temperature resistance point of view.

2. Experimental procedure

Commercially available α-SiC (UF10, H.C. Starck, Germany), AlN (Pyrofine A, Atochem, France) and Y_2O_3 (H.C. Starck, Germany) were used as starting powders. Characteristics of these powders are reported in Table 1.

A batch of powder composed by 48 wt.% SiC, 48 wt.% AlN and 4 wt.% Y_2O_3 was wet-mixed in ethanol for 12 h using SiC grinding balls. After drying and sieving, the powder was compacted by die pressing at 67 MPa and was subsequently pressed at 150 MPa by CIP.

Sintering was performed in a graphite elements furnace in flowing nitrogen at 1 atm with green bodies put inside a graphite crucible without powder bed. Sintering was performed at 1950 °C for 30 min, while an annealing step was conducted at 2050 °C.

The bulk densities of the sintered samples were determined using the Archimede method. The microstructures were characterized using scanning electron microscopy (SEM), while X-ray diffractometry (XRD) using Cu Kα radiation was performed in order to determine the crystallographic composition of the sintered samples before and after the oxidation treatments.

Oxidation experiments were carried out at different temperatures in the range 1200–1500 °C over a period of 200 h in air. Rectangular pellets (11 mm × 12 mm × 8 mm) were prepared from the bulk specimen with a diamond saw. After grounding to reduce superficial roughness, the specimens were cleaned in an ultrasonic bath and degreased with acetone and ethanol. Dried samples were then weighed and the exact dimensions were measured in order to calculate the surface area. The experiments were conducted in a furnace having molybdenum disilicide heating elements.

3. Results and discussion

3.1. Sintering and microstructure

Bulk density of the sintered samples was 98%T.D. Residual porosity was due to the weight loss associated to the formation of gaseous products of redox reactions between SiC and SiO_2, Al_2O_3 or Y_2O_3:

$$SiC + 2SiO_2 \Leftrightarrow CO_{(g)} + 3SiO_{(g)} \quad (1)$$

$$SiC + Al_2O_3 \Leftrightarrow CO_{(g)} + SiO_{(g)} + Al_2O_{(g)} \quad (2)$$

$$SiC + 2Y_2O_3 \Leftrightarrow CO_{(g)} + SiO_{(g)} + 4YO_{(g)} \quad (3)$$

Total weight loss associated to the sintering was experimentally determined equal to 2.5 wt.%. Previous work focused on the study of LPS-SiC clearly showed that the main contribution to the weight loss comes from reactions (1) and (2), while weight loss is not greatly influenced by the decomposition of yttria (reaction (3)).[18] In fact, among the species present in the sample, yttria is the most thermodynamically stable one and unlikely to decompose under carbothermally reducing conditions at temperatures up to 2000 °C.[19] On the other hand, yttria participates to the formation of $Y_{10}Al_2Si_3O_{18}N_4$, which has frequently been detected with Y_2O_3–AlN as sintering additives.[20,21] In our case, this crystalline phase acts as liquid phase that assists densification during pressureless sintering[10] and precipitates at the grain boundary during cooling. This phase was detected as secondary phase with XRD analysis, while 2H SiC–AlN solid solution and α-SiC were identified as major crystalline phases (Fig. 1). Minor crystalline phases are identified to be SiO_2 (cristobalite) and Al_2SiO_5 (andalusite).

Furthermore, SEM micrograph, obtained with back-scattered electrons and reported in Fig. 2, put in evidence the bright spots of the liquid phase having a higher average atomic number and revealed that the grain boundary phase $Y_{10}Al_2Si_3O_{18}N_4$ is homogenously distributed in the sample. This fact confirms that we are able to control the weight loss during sintering even though a powder bed to protect the green bodies is not used.[18] Additional microstructural investigation was performed after plasma etching (70% CF_4–30% O_2 for 30 min). The method of plasma etching has mainly been used for Si-based compounds (Si_3N_4, SiAlON, SiC) and it is particularly indicated for liquid phase sintered ceramics. In the case of SiC–AlN composites, plasma etching is useful to put in evidence SiC grains and grain boundary phases, while 2H solid solution is not etched by plasma.[22] It is clearly showed in the micrograph reported in

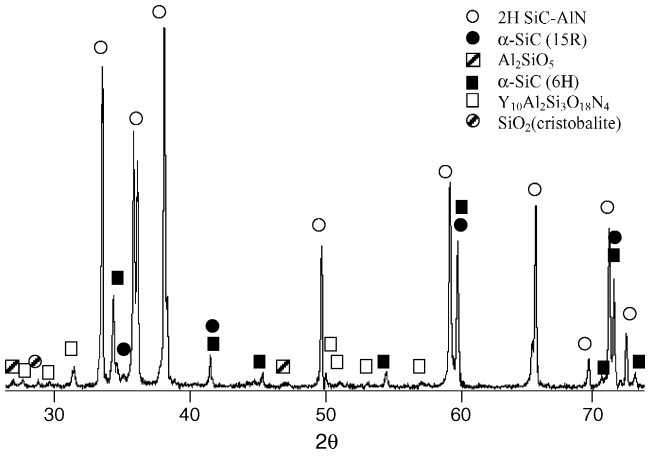

Fig. 1. XRD pattern of 50 wt.%SiC–50%AlN composite pressureless sintered without powder bed.

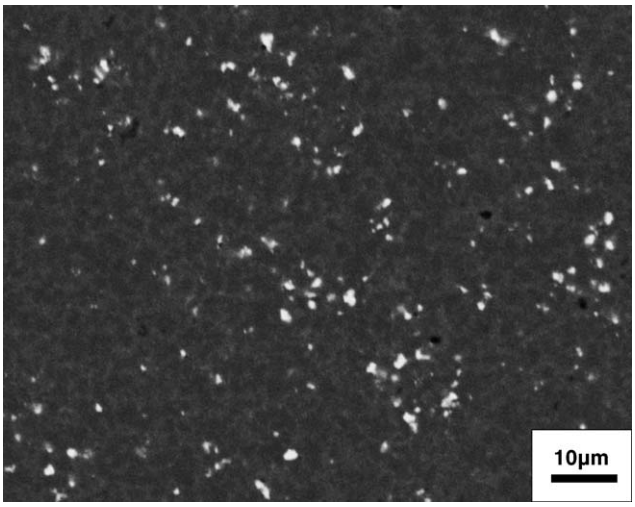

Fig. 2. SEM back-scattered electrons image of the sintered SiC–AlN composite.

Fig. 3, where dispersed SiC grains (indicated by arrow B) and solidified liquid phase (indicated by arrows C) could be qualitatively distinguished from 2H solid solution (indicated by arrow A) by means of EDS X-ray microprobe analysis (Fig. 4). In addition, EDS pattern of 2H solid solution reported in Fig. 4a shows that the AlN content is higher than that of SiC. This fact was already interpreted by Lee et al.[22] as indication that the SiC diffusion rate in the AlN grains is faster than that of AlN in the SiC grains.

3.2. Oxidation behaviour

Fig. 5 shows the relation between the square of the weight gain and the oxidation time for specimens oxidized in air at temperature between 1200 and 1500 °C. For all temperatures, oxidation kinetics were of the parabolic type. Thus, the oxidation behaviour is governed by the parabolic rate equation:

$$\Delta W^2 = kt \tag{4}$$

where ΔW is the specific weight gain, k is the kinetic constant of parabolic oxidation and t is the oxidation time.

On the basis of Eq. (4), parabolic rate constants for each temperature were determined from the slope of the straight lines

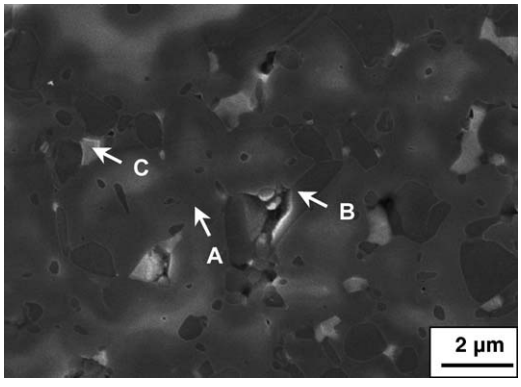

Fig. 3. SEM micrograph of plasma etched surface of the sintered SiC–AlN composite.

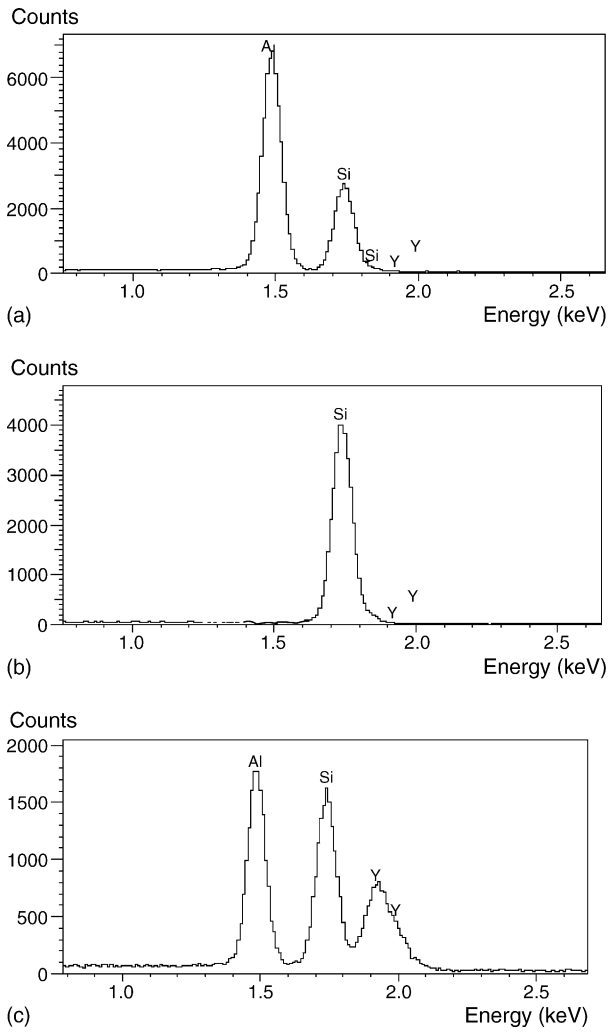

Fig. 4. EDS spectra of (a) SiC–AlN solid solution indicated by A in Fig. 3; (b) SiC grain indicated by B in Fig. 3 and (c) $Y_{10}Al_2Si_3O_{18}N_4$ indicated by C in Fig. 3.

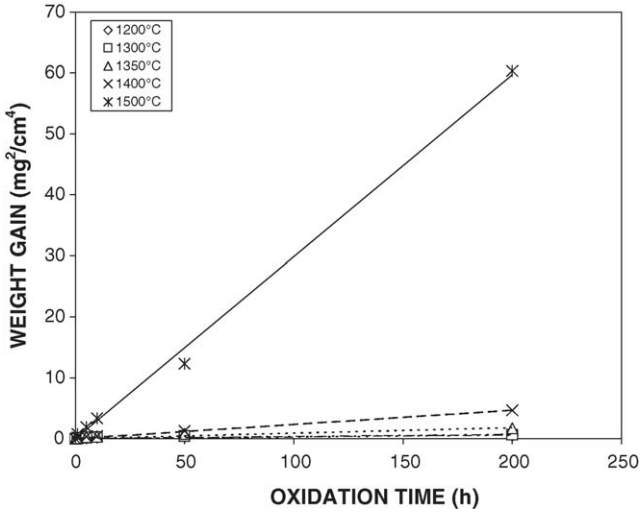

Fig. 5. Square of the weight gains as a function of time at 1200, 1300, 1350, 1400 and 1500 °C.

Table 2
Comparison of the weight gains and parabolic rate constants (k) of the SiC–AlN composite developed in this study with those of SiC–AlN materials obtained by other authors

Reference	Sintering	Additive	SiC/AlN weight ratio	Weight gain (mg/cm^2)	Parabolic rate constant (kg^2 m^{-4} s^{-1})
This study	LPPS without powder bed	Y_2O_3	50/50	0.50 (1200 °C, 200 h) 0.80 (1300 °C, 200 h) 1.30 (1350 °C, 200 h) 2.16 (1400 °C, 200 h) 7.77 (1500 °C, 200 h)	5.63×10^{-12} (1200 °C) 1.00×10^{-10} (1300 °C) 2.50×10^{-10} (1350 °C) 6.53×10^{-10} (1400 °C) 8.29×10^{-9} (1500 °C)
Lavrenko et al.[23]	Hot pressing		50/50	1.5 (1350°, 6 h)	0.9×10^{-8} (1350 °C)
Sciti et al.[16]	LPPS with powder bed	Y_2O_3	22/78	2.79 (1350 °C, 30 h) 10.75 (1400 °C, 30 h)	7.3×10^{-9} (1350 °C) 1.1×10^{-7} (1400 °C)
Choi et al.[24]	Hot pressing	Y_2O_3	97/3	1.99 (1400 °C, 192 h)	3.67×10^{-9} (1400 °C)
Pan et al.[25]	Hot pressing	Y_2O_3	85/15	3.00 (1370 °C, 30 h)	n.d.

reported in Fig. 5. The values of specific weight gains and parabolic rate constants are summarized in Table 2 together to the experimental data of other SiC–AlN composites manufactured in different conditions.[16,23–25] These results indicate that the oxidation resistance of SiC–AlN ceramics pressureless sintered without powder bed can be compared with that of SiC–AlN composites obtained with more expensive sintering processes. In particular, it is interesting to note that our material presents a specific weight gain (and a parabolic rate constant) lower than hot isostatic pressed material manufactured without sintering-aid.

Parabolic oxidation behaviour of ceramics normally indicates that the rate-determining step is a diffusional process associated with the migration of ions.[26] In the case of solid state sintered SiC, Luthra[27] reviewed many studies on oxidation of SiC and concluded that, although most observed parabolic oxidation rate, mixed diffusion/reaction rate mechanism must be controlling the oxidation of SiC. Recently, Biswas et al.[28] found high activation

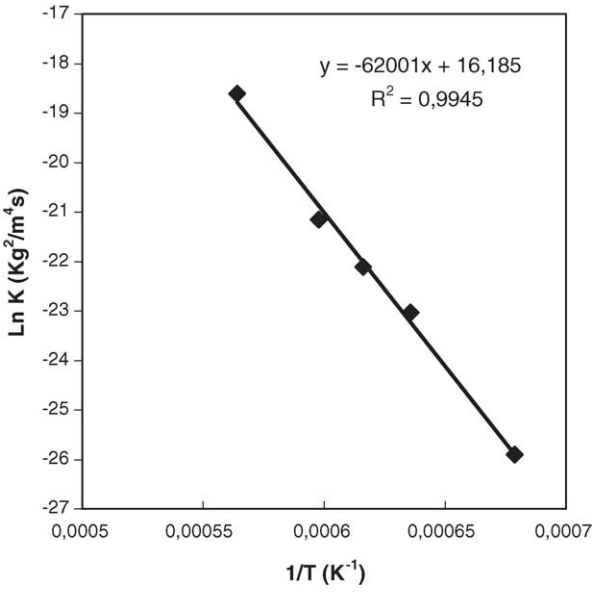

Fig. 6. Arrhenius plot of parabolic rate constants for oxidation in the temperature range 1200–1500 °C.

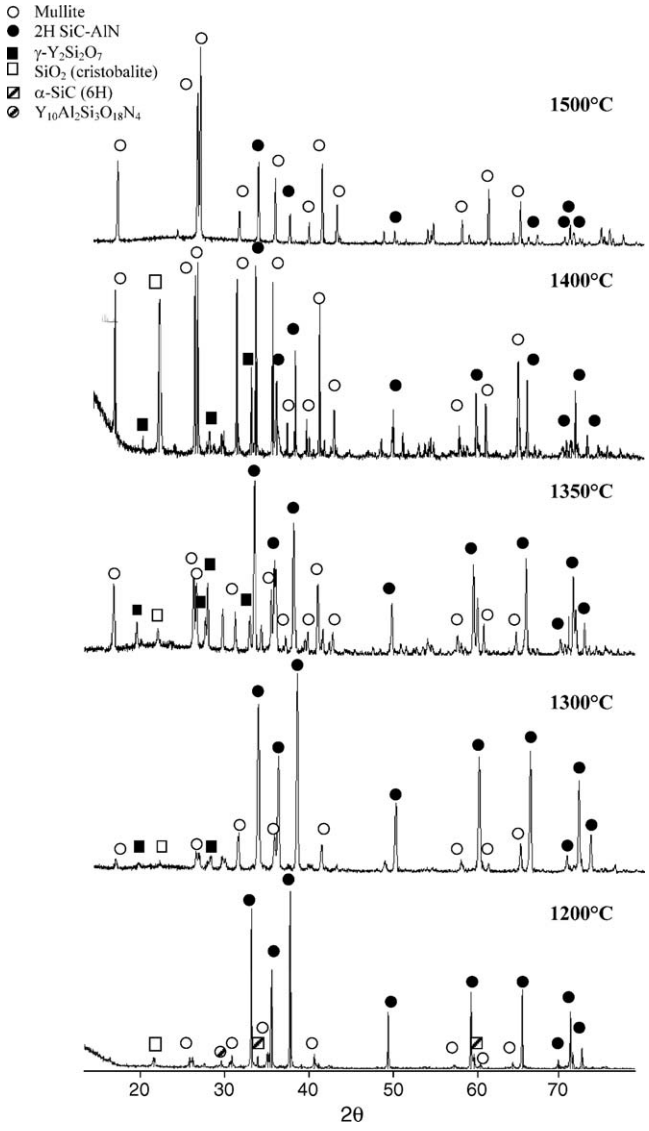

Fig. 7. XRD patterns of the oxidized surface of SiC–AlN composite.

energies (250–560 kJ/mol) for the oxidation process in lutetia-doped SiC–AlN composites and consequently suggested that oxidation proceeds not only by the diffusion of oxygen through the silica layer, but also by interfacial reactions between the growing silica layer and lutetia. On the basis of the parabolic rate constants reported in Table 2, we were able to determine the activation energy between 1200 and 1500 °C on the basis of the Arrhenius law:

$$k = k_0 \exp\left(-\frac{Q}{RT}\right) \tag{5}$$

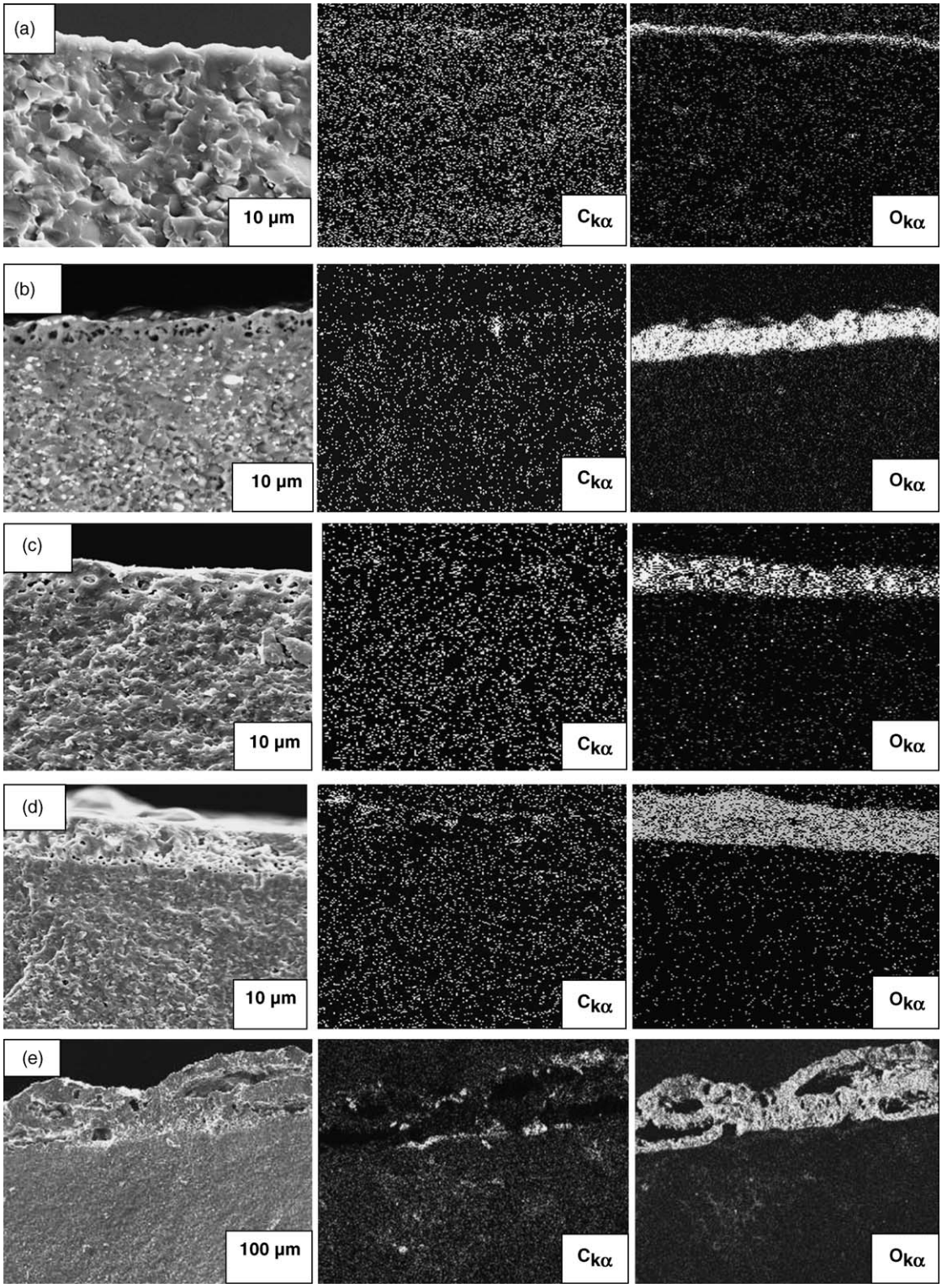

Fig. 8. SEM micrographs, carbon and oxygen X-ray mapping of the cross-sections of the oxidized specimens at (a) 1200 °C; (b) 1300 °C; (c) 1350 °C; (d) 1400 °C; and (e) 1500 °C for 200 h.

where k_0 is a material constant, Q is the oxidation activation energy, T is the absolute temperature and R is the gas constant. The apparent oxidation activation energy, calculated from the slope of the straight line reported in Fig. 6, was found to be 515 kJ/mol, higher than the activation energy associated to the diffusion of oxygen both through the silica (150 kJ/mol)[28] and mullite layer (260–290 kJ/mol).[29] This value suggests that not only the diffusion of oxygen through the silica-based surface oxide scale have to be considered as rate-controlling mechanism, but also the interfacial reactions between SiO_2 and Al_2O_3, oxidation products of SiC and AlN, which led to the formation of mullite:

$$SiC_{(s)} + \tfrac{3}{2}O_{2(g)} \Leftrightarrow SiO_{2(s)} + CO_{(g)} \quad (6)$$

$$4AlN_{(s)} + 3O_{2(g)} \Leftrightarrow 2Al_2O_{3(s)} + 2N_{2(g)} \quad (7)$$

$$2SiO_{2(s)} + 3Al_2O_{3(s)} \Leftrightarrow 3Al_2O_3{\cdot}2SiO_{2(s)} \quad (8)$$

Lavrenko et al.[15] demonstrated that mullite and SiO_2 (α-cristobalite) were the main constituents of the surface scale of 50/50 weight ratio SiC–AlN composites oxidized at 1500 °C for 6 h. In our case, XRD analysis performed on the oxidized surface after oxidation in the range 1200–1500 °C for 200 h confirmed that the main oxidation products were mullite and silica, but with $T > 1200$ °C yttrium disilicate (γ-$Y_2Si_2O_7$) was also found in the oxide scale as reported in Fig. 7.

After oxidation at 1200 °C, α-cristobalite and mullite were only formed (reactions (6)–(8)) and 2H solid solution SiC–AlN was detected as major phase (6H-SiC was also found). At this temperature grain boundary phase ($Y_{10}Al_2Si_3O_{18}N_4$) was also identified, but its content was lower than that of the as-sintered sample.

At higher temperature (≥1300 °C), γ-$Y_2Si_2O_7$ was likely formed from the decomposition of the grain boundary phase,[30] while α-cristobalite and mullite contents increased. At 1500 °C, mullite and 2H solid solution were detected. Cristobalite was not detected because of SiC oxidation at very high temperature (≥1500 °C) proceeds on the basis of the following reactions[31–33]:

$$SiC_{(s)} + O_{2(g)} \Leftrightarrow SiO_{(g)} + CO_{(g)} \quad (9)$$

$$SiC_{(s)} + O_{2(g)} \Leftrightarrow SiO_{2(g)} + C_{(s)} \quad (10)$$

$$SiO_{2(s)} + C_{(s)} \Leftrightarrow SiO_{(g)} + CO_{(g)} \quad (11)$$

While reaction (6) represents the SiC "passive" oxidation, reactions (9)–(11) describe the SiC "active" oxidation.[32,33] Therefore, at very high temperature, α-cristobalite, formed by means of reactions (6) and (10), reacted with alumina, produced by reaction (7), to obtain mullite (reaction (8)). At the same time, SiO_2 also reacted with graphite, produced by reaction (10), to obtain volatile species SiO and CO (reaction (11)). Residual graphite coming from reaction (10) was revealed by SEM-EDS at the interface between oxide layer and substrate in the sample oxidized at 1500 °C for 200 h (see the carbon X-ray map of Fig. 8e). The occurrence of graphite was already reported in previous studies focused on the oxidation of Al_2O_3–SiC whiskers composites,[34] Al_2O_3–ZrO_2–SiC_w composites[35] and hot pressed 37 wt.% SiC–63 wt.%AlN.[36] In our case, this confirms that the SiC oxidation mechanism changes from "passive" to "active" at very high temperature (≥1500 °C) following the reaction sequences proposed in this paragraph. An additional consequence of the SiC "active" oxidation is the formation of gaseous species, SiO and CO. The formation of these compounds caused the creation of defects (holes, bubbles) in the oxide layer as reported in Fig. 8e. In this figure the SEM micrograph of the cross section of the sample oxidized at 1500 °C for 200 h is shown. This sample presents an oxide layer of 100–150 μm unable to act as protective barrier against oxygen diffusion as confirmed by the EDS oxygen X-ray map. On the contrary, same analysis performed on the samples oxidized in the range 1200–1400 °C confirmed that the thin oxide layer (from 5 μm at 1200 °C up to 20 μm at 1400 °C), composed mainly by mullite, is able to improve the oxidation resistance of pressureless sintered 50 wt.%SiC–50 wt.%AlN composites.

4. Conclusion

50 wt.%SiC–50 wt.%AlN composite can be pressureless sintered without powder bed with Y_2O_3 as sintering aid. Oxidation resistance of this material in the temperature range 1200–1500 °C is comparable with that of SiC–AlN composites obtained by means of more expensive sintering processes. In particular, the detail analysis of the parabolic oxidation behaviour showed that the kinetic of the oxidation process is quite complex and is not only controlled by the diffusion of oxygen through the oxidized layer, but also by surface reactions. The oxide layer is mainly formed by mullite and cristobalite at 1200 °C, while yttrium disilicate is also detected at temperature higher than 1200 °C. The oxide scale represents an efficient barrier against oxygen diffusion in the temperature range 1200–1400 °C, while at higher temperature (1500 °C) it presents large porosity due to the "active" oxidation of SiC.

Acknowledgements

The authors acknowledge the Italian Minister for University and Scientific Research for the financial support under project "PUMA". Furthermore, the authors wish to thank C. Mingazzini and L. Pilotti (ENEA, Faenza, Italy) for the XRD and SEM-EDS analysis, respectively, and F. Monteverde and A. Balbo (CNR-ISTEC Faenza, Italy) for the plasma etching.

References

1. Cutler, I. B., Miller, P. D., Rafaniello, W., Park, H. K., Thompson, D. P. and Jack, K. H., New materials in the Si–C–Al–O–N and related system. *Nature*, 1978, **V**(275), 434.
2. Ruh, R. and Zangvil, A., Composition and properties of hot-pressed SiC–AlN solid solution. *J. Am. Ceram. Soc.*, 1982, **65**(5), 260–265.
3. Rafaniello, W., Cho, K. and Virkar, V. A., Fabrication and characteristics of SiC–AlN alloys. *J. Mater. Sci.*, 1981, **16**, 3479–3488.
4. Jou, Z. C., Virkar, V. and Cutler, A. R., High temperature creep of SiC densified using a transient liquid phase. *J. Mater. Res.*, 1991, **6**(9), 1945–1949.

5. Zangvil, A. and Ruh, R., Phase relationship in the silicon carbide-aluminum nitride system. *J. Am. Ceram. Soc.*, 1988, **71**(10), 884–890.
6. Mandal, S., Dhargupta, K. K. and Ghatak, S., Gas pressure sintering of SiC–AlN composites in nitrogen atmosphere. *Ceram. Int.*, 2002, **28**, 145–151.
7. Lee, R. R. and Wei, W., Fabrication, microstructure and properties of SiC–AlN ceramic alloys. *Ceram. Eng. Sci. Proc.*, 1990, **11**(7–8), 1094–1121.
8. Miura, M., Yogo, T. and Hirano, S. I., Phase separation and toughening of SiC–AlN solid-solution ceramics. *J. Mater. Sci.*, 1993, **28**, 3859–3865.
9. Li, J. F. and Watanabe, R., Pressureless sintering and high-temperature strength of SiC–AlN ceramics. *J. Ceram. Soc. Japan*, 1994, **102**(8), 727–731.
10. Magnani, G. and Beaulardi, L., Properties of liquid phase pressureless sintered SiC-based materials obtained without powder bed. *J. Aus. Ceram. Soc.*, 2005, **41**(1), 31–36.
11. Xu, Y., Zangvil, A., Landon, M. and Thevenot, F., Microstructure and mechanical properties of hot-pressed silicon carbide-aluminum nitride composition. *J. Am. Ceram. Soc.*, 1988, **75**(2), 325–333.
12. Landon, M. and Thevenot, F., The SiC–AlN system: influence of elaboration routes on the solid solution formation and its mechanical properties. *Ceram. Int.*, 1991, **17**, 97–110.
13. Kobayashi, Y., Li, J. F., Kawasaki, A. and Watanabe, R., Microstructure and high-temperature property of reaction HIP-sintered SiC–AlN ceramic alloys. *Mater. Trans.*, 1996, **37**(4), 807–812.
14. Lim, C. S., Effect of a-SiC on the microstructure and toughening of hot-pressed SiC–AlN solid solution. *J. Mater. Sci.*, 2000, **35**, 3029–3035.
15. Lavrenko, V. A., Desmanion-Brut, M., Panasyuk, A. D. and Desmanion, J., Features of corrosion resistance of AlN–SiC ceramics in air up to 1600 °C. *J. Eur. Ceram. Soc.*, 1998, **18**, 2339–2343.
16. Sciti, D., Winterhalter, F. and Bellosi, A., Oxidation behaviour of pressureless sintered AlN–SiC composite. *J. Mater. Sci.*, 2004, **39**, 6965–6973.
17. Pan, Y. B., Qiu, J. H., Kawagoe, M., Morita, M., Tan, S. H. and Jiang, D. L., SiC–AlN particulate composite. *J. Eur. Ceram. Soc.*, 1999, **19**, 1789–1793.
18. Grande, T., Sommerset, H., Hagen, E., Wiik, K. and Einarsud, M., Effect of weight loss on liquid-phase-sintered silicon carbide. *J. Am. Ceram. Soc.*, 1997, **80**(4), 1047–1052.
19. Rixecker, G., Biswas, K., Wiedmann, I. and Aldinger, F., Liquid-phase sintered SiC ceramics with oxynitride addittives. *J. Ceram. Process. Res.*, 2000, **1**(1), 12–19.
20. Schneider, J., Biswas, K., Rixecker, G. and Aldinger, F., Microstructural changes in liquid-phase-sintered silicon carbide during creep in an oxidizing environment. *J. Am. Ceram. Soc.*, 2003, **86**(3), 501–507.
21. Ye, H., Rixecker, G., Haug, S. and Aldinger, F., Compositional identification of the intergranular phase in liquid phase sintered SiC. *J. Eur. Ceram. Soc.*, 2002, **22**, 2379–2387.
22. Lee, J. K., Tanaka, H. and Kim, H., Formation of solid solutions between SiC and AlN during liquid-phase sintering. *Mater. Lett.*, 1996, **29**, 1–6.
23. Lavrenko, V. A., Baxter, D. J., Panasyuk, A. D. and Desmanion-Brut, M., High-temperature corrosion of AlN-based composite ceramic in air and in combustion products of commercial fuel. I. Corrosion of ceramic composites in the AlN-SiC system in air and in combustion products of kerosene and diesel fuel. *Powder Metall. Metal Ceramics*, 2004, **43**(3–4), 179–186.
24. Choi, H. J., Lee, J. G. and Kim, Y. W., Oxidation behaviour of liquid-phase sintered silicon carbide with aluminium nitride and rare-earth oxides (Re_2O_3, where Re = Y, Er, Yb). *J. Am. Ceram. Soc.*, 2002, **85**(9), 2281–2286.
25. Pan, Y. B., Qiu, J. H. and Morita, M., Oxidation and microhardness of SiC–AlN composite at high temperature. *Mater. Sci. Bull.*, 1998, **33**(1), 133–139.
26. Singhal, J. S. C., Thermodynamics and kinetics of oxidation of hot-pressed silicon nitride. *J. Mater. Sci.*, 1976, **11**, 500–509.
27. Luthra, K. L., Some new perspective on oxidation of silicon carbide and silicon nitride. *J. Am. Ceram. Soc.*, 1991, **74**(5), 1095–1103.
28. Biswas, K., Rixecker, G. and Aldinger, F., Effect of rare-earth cation additions on the high temperature oxidation behaviour of LPS-SiC. *Mater. Sci. Eng. A*, 2004, **374**, 56–63.
29. Fritze, H., Jojic, J., Witke, T., Ruscher, C., Weber, S., Scherrer, S., Weiss, R., Schultrich, B. and Borchardt, G., Mullite based oxidation protection for SiC–C/C composites in air at temperatures up to 1900K. *J. Eur. Ceram. Soc.*, 1998, **18**, 2351–2364.
30. Rixecker, G., Wiedmann, I., Rosinus, A. and Aldinger, F., High-temperature effects in the fracture mechanical behaviour of silicon carbide liquid-phase sintered with AlN–Y_2O_3 addittives. *J. Eur. Ceram. Soc.*, 2001, **21**, 1013–1019.
31. Filsinger, D. H. and Bourrie, D. B., Silica to silicon: key carbothermic reactions and kinetics. *J. Am. Ceram. Soc.*, 1990, **73**(6), 1726–1732.
32. Gulbrunsen, E. A. and Jansonn, S. A., The high-temperature oxidation, reduction, and volatilization reactions of silica and silicon carbide. *Oxid. Met.*, 1972, **4**, 181–201.
33. Ervin, G., Oxidation behaviour of silicon carbide. *J. Am. Ceram. Soc.*, 1968, **41**, 347–352.
34. Lin, F., Marieb, T., Morrone, A. and Nutt, S., Thermal oxidation of Al_2O_3–SiC whiskers composites: mechanism and kinetics. In *Materials Research Society Symposia Proceedings, vol. 120, High Temperature/High Perfomance Composites*, ed. F. D. Lemkey, A. G. Evans, S. C. Fishmann and J. R. Strife. Materials Research Society, Pittsburgh, PA, 1988, pp. 327–331.
35. Backhaus-Ricoult, M., Oxidation behaviour of SiC-whisker-reinforced-alumina-airconia composites. *J. Am. Ceram. Soc.*, 1991, **74**(8), 1793–1803.
36. Xu, Y. and Zangvil, A., Formation of beta-SiAlON as an intermediate oxidation product of SiC–AlN ceramics. *J. Am. Ceram. Soc.*, 1995, **78**(10), 2753–2762.